Theor Chem Acc (2004) 111:141–153
DOI 10.1007/s00214-003-0539-y

Theoretical
Chemistry Accounts

Regular article

Towards a modellisation of the solvation energy in multi-component solvents. The interesting case of a charged solute imbedded in a polymer-containing electrolyte solution

Antonio Raudino

Dipartimento di Scienze Chimiche, Università di Catania, Viale A. Doria 6, 95125 Catania, Italy

Received: 15 March 2003 / Accepted: 30 April 2003 / Published online: 8 December 2003

Abstract. In this paper we propose a mean-field theory to calculate the solvation free energy of a charged solute imbedded in a complex multi-component solvent. We considered a solvent made up of a mixture of small (electrolyte solution) and large (polymer) components. The presence of macromolecules ensures reduced mixing entropy among the different solvent components, an effect due to polymer connectivity. The reduced entropy favours strong preferential distribution of a particular solvent even in the presence of weak preferential solute–solvent interactions. In addition, two energy terms must be considered: (a) the interaction between the solute electrostatic potential and the electrolyte solution and (b) the formation of a polymer–solute interface. Because of the different dielectric permittivity of the solvent components, the electrolyte and polymer distribution functions are strongly coupled: ions, indeed, are more solvated in regions of higher local dielectric permittivity arising from the inhomogeneous mixing of solvent and polymer. We combined together the different energy terms in the framework of the de Gennes free energy functional for polymer solutions along with a generalised Poisson–Boltzmann equation developed for inhomogeneous dielectric media. Moreover, the preferential electrolyte solvation in regions of greater polarity was considered by an extension of the Born equation.Setting the polymer dielectric permittivity smaller than the solvent one and making null the specific polymer–solute interactions, we calculated enhanced electrolyte concentration and reduced polymer concentration near the solute surface on raising the solute surface charge density. The theory shows also the breakdown of the widely used separation between electrostatic and surface tension-dependent contributions to solvation energy when non-ideal mixed solvents are considered. In fact, according to the model, the surface tension of such mixed solvents strongly depends on the solute surface charge density: at high potentials the interfacial tension may increase rather than decrease on raising the polymer volume fraction. The theoretical results have been compared with experimental data on polymer + electrolyte solution surface tension and with solubility data of colloidal particles.The comparison evidences the complex behaviour of multi-component solvents going well beyond the trivial weighted average of the dielectric permittivity and surface tension of the isolated chemical components. Deviations from the simple behaviour predicted by an average picture of multi-component solvents could be understood by developing more sophisticated, but still simple, approaches like that proposed in this paper.

Keywords: Solvation energy – Mixed solvents – Polymers – Continuum picture of the solvent – Dielectric permittivity – Poisson–Boltzmann equation

Contribution to the Jacopo Tomasi Honorary Issue.This paper is dedicated to Jacopo Tomasi. I learned much of the difficult art of transforming complex problems into simple models after reading his early works on solvation energy.

e-mail: araudino@dipchi.unict.it

Introduction

A continuum picture of the solvent around a solute particle is extremely appealing because it reduces the complex many-body problem typical of solute–solvent interactions to a pseudo two-body one. Among the different continuum theories, particularly simple and useful appear to be those based on a classical electrostatics picture of the solvent depicted as a continuum and homogeneous dielectric surrounding a solute-containing cavity. Inside the cavity, whose size and shape are proportional to that of the bare solute molecule, the charge distribution of the solute polarises the cavity interface. In turn, the induced electrostatic potential interacts with the solute, inducing charges. The free energy associated with the charging process described above represents the

electrostatic contribution to the solvation energy, a concept thoroughly developed in many papers either in a classical or a quantistic description of the solute [1, 2]. The work needed to create a solute-containing cavity inside the solvent is usually named cavitation (or solvophobic) energy. This contribution, to be added to the electrostatic one, is roughly proportional to the solute–solvent interfacial area and to the solvent interfacial tension (see, e.g. [2, 3] and references therein).

Dielectric continuum models developed so far basically deal with the following systems: (i) one-component neutral solvents, and (ii) neutral solvents where point-like charges are dissolved (electrolyte solution). Mixtures of neutral solvents could be approximately described by introducing the averaged dielectric permittivity and interfacial tension, which are roughly the weighted average of the isolated solvent properties. Such a naive picture completely neglects the notion of preferential solvation or, in other words, the different radial distribution of the two solvents around the solute (for a series of recent representative papers on this topic see, e.g., [4, 5, 6, 7]). Preferential solvation for a specific solvent may induce strong deviation of the solvation energy calculated by using weighted average properties of the mixed solvent.

Multi-component solvents represent an interesting field, quite unexplored by theoreticians. Particularly interesting are those with huge differences in size, for instance water (or electrolyte solutions) and water-soluble polymers. The interest in such a kind of mixed solvent is two-fold:

(a) From a fundamental point of view the above system strongly deviates from the ideal behaviour because the solvent entropy is dramatically lowered when large molecules are mixed with small ones (see the forthcoming section for a more quantitative analysis). This means that even modest preferential interactions of one solvent with the solute may locally change the mixing properties giving rise to a sort of local phase separation just near the solute–solvent interface. When large solutes are considered, this picture allows one to introduce concepts like wetting transitions or hydrodynamic instability of stratified fluids, probably useful in describing solvation energy in multicomponent fluids.

(b) Most key biological structures (e.g. cells, vesicles, viruses, platelets and chromosomes) are micron-sized charged objects imbedded in an electrolyte solution also containing water-soluble macromolecules (hydrosoluble proteins, mucopolysaccharides and so on). Furthermore, in recent years there has been a growing technological interest in water-based solvents made up of electrolyte solutions and water-soluble polymers [8] (e.g. polyethylene glycol (PEG)). These fluids do not contain volatile solvents, dangerous for human health and harmful to the environment; moreover, by varying the kind and/or concentration of electrolytes one can continuously shift their solvophobic and solvophilic properties. For instance, dilute PEG–electrolyte aqueous solutions are currently used in biotechnological laboratories to induce aggregation and fusion of cells, viruses and lipid vesicles [9, 10], to condense highly charged macromolecules like DNA [11] or in protein crystallisation procedures [12].

On the basis of these considerations it should be interesting to investigate by simplified models the complex interplay between solute–electrolyte and solute–polymer interactions that, as we will show later, are strongly coupled to each other in a rather intricate way.

Theory

Free energy functional

Consider a dilute electrolyte solution in which a neutral, soluble polymer is dissolved. We focus the analysis on physical conditions where the two components (electrolyte solution and polymer) do not phase-separate in the whole range of considered concentrations and temperature. The model is developed in the case of large solutes whose size is larger than the polymer gyration radius; the opposite limit of small solutes must be treated by adopting a completely different picture [13, 14].

Letting z be the distance from the solute surface (considered as an infinite plane, curvature effects are here ignored), we define $c_+(z)$ and $c_-(z)$ as the local concentration of positive and negative ions, each of them carrying a positive and negative charge $\pm Ze$, respectively (symmetrical electrolyte). Moreover, $\Phi(z)$ is the local polymer volume fraction and $N>>1$ the polymerisation degree. The corresponding polymer and electrolyte bulk concentrations are denoted $\bar{\Phi}$ and $\bar{c}_+ = \bar{c}_- = \bar{c}$. Mass conservation imposes the following relationship to the solvent mole fraction: $\bar{\Phi}_s = 1 - \bar{\Phi} - 2\bar{c} \approx 1 - \bar{\Phi}$ in dilute electrolyte solutions. In the following we explore the relevant case of semi-dilute polymer solutions, defined over the concentration range [15]

$$N^{-4/5} << \bar{\Phi} << 1 \tag{1}$$

In this range coils do overlap but the polymer fraction is still low, a situation which allows for a useful continuum picture of the polymer solution. At lower concentrations (dilute regime) coils behave like an ideal gas of isolated hard spheres of radius $R_F\left(\approx N^{-3/5}\right)$ and the picture of polymer–surface interaction somewhat resembles the well-known Langmuir adsorption isotherm. A cartoon of the investigated system is given in Fig. 1.

In a mean-field picture the free energy of a polymer semi-dilute solution can be partitioned as follows. The

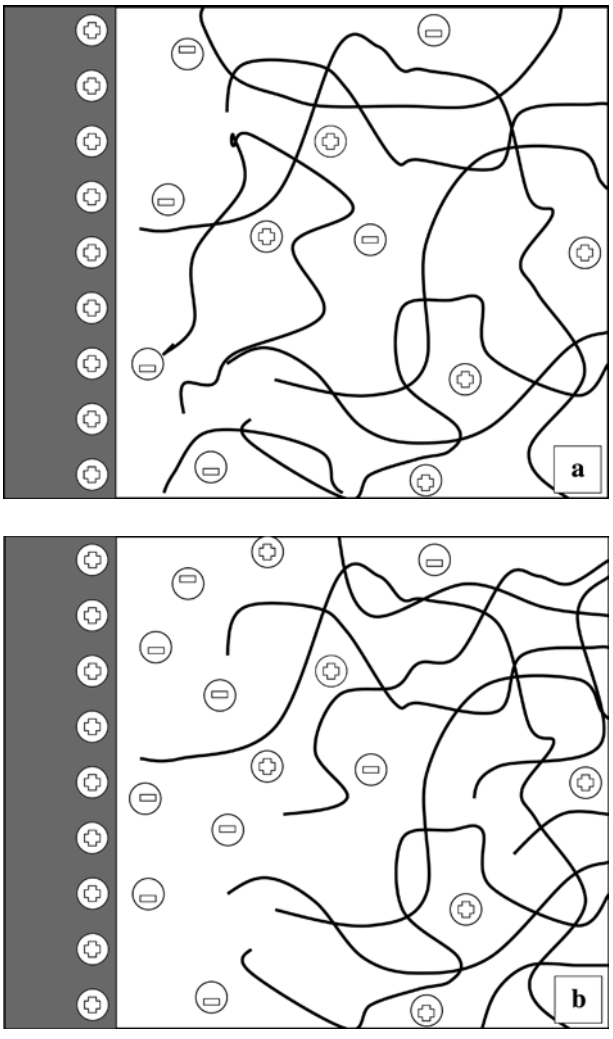

Fig. 1. Schematic drawings of a polymer-containing electrolyte solution in contact with a charged wall in the presence (**a**) and in the absence (**b**) of polymer–ion coupling

entropic contribution to the free energy associated with homogeneous mixing among polymer, solvent and ions reads

$$-T\Delta S_{\mathrm{MIX}}^{\mathrm{hom}} \approx kT\frac{1}{a^3}\int_V \left(\frac{\Phi(z)}{N}\log\frac{\Phi(z)}{N} + c_+(z)\log c_+(z) + c_-(z)\log c_-(z) + (1-\Phi(z))\log(1-\Phi(z))\right)dV \tag{2}$$

where k is the Boltzmann constant, T is the absolute temperature and a is the size (length) of the single molecular units (monomers, ions and solvent) which, for the sake of compactness, have been assumed to have identical size, a generalisation to the case of different sizes being straightforward. The integration is extended over the volume V of the electrolyte solution.

Equation 2 applies to nearly homogeneous polymer solutions. In the presence of concentration gradients an additional term must be considered. The occurrence of spatial heterogeneities in fact modifies the whole energy of fluid solutions, both for enthalpic and entropic contributions. However, at variance with small-sized molecular fluids, where the effects of concentration gradients are localised near the interface, in strongly correlated systems like polymer solutions, the perturbation propagates deep inside the fluid. In semi-dilute polymer solutions a fairly good expression for this term reads

$$-T\Delta S_{\mathrm{MIX}}^{\mathrm{inhom}} \approx kT\frac{1}{a^3}\int_V \frac{a^2}{24\Phi(z)(1-\Phi(z))}\left(\frac{\partial\Phi(z)}{\partial z}\right)^2 dV \tag{3}$$

Different theories for inhomogeneous polymer solutions do not appreciably modify the above result, the only variation occurring in the numerical coefficient [15, 16, 17].

The interaction energy among solvent, polymer and ions can be decomposed into the sum of two different terms. The former is the classical Flory-type contribution accounting for polymer–polymer, polymer–solvent and solvent–solvent forces [15]. They can be described in a mean-field picture through a single dimensionless parameter $\chi = \chi(T) \equiv \frac{1}{2kT}\left(-W_{\mathrm{ss}} - W_{\mathrm{pp}} + 2W_{\mathrm{sp}}\right)$, where W_{ij} describes the pair interaction energy between i-th and j-th chemical species (in most cases $\chi > 0$). Following this picture, the whole energy of interaction takes the simple form $kT\frac{1}{a^3}\chi\int_V \Phi(z)(1-\Phi(z))dV$.

The second term describes the solvation energy of positive and negative ions imbedded in a heterogeneous medium (solvent + ions + polymer). In the simplest case of a homogeneous fluid this contribution can be evaluated in a continuum picture by knowing the averaged dielectric permittivity $\bar{\varepsilon} \equiv \varepsilon(\bar{\Phi})$ and electrolyte concentration $\bar{c}$. Standard electrostatics yields a Born-like equation $E_{\mathrm{ION}} = -\frac{Z^2e^2}{2a}\left(1 - \frac{1}{\bar{\varepsilon}(1+\bar{\kappa}a)}\right)$, where $\bar{\kappa} \equiv \left(\frac{8\pi Z^2e^2\bar{c}}{\bar{\varepsilon}kT}\right)^{1/2}$ is the inverse of the Debye length. The above formula, whose proof can be found in electrochemical textbooks [18], can be easily generalised to the case of a space-varying ion distribution inside a heterogeneous dielectric medium, a situation occurring for instance near a solute–solvent interface: $E_{\mathrm{ION}} = -\frac{Z^2e^2}{2a}\frac{1}{a^3}\int_V \left(1 - \frac{1}{\varepsilon(\Phi(z))(1+\kappa(z)a)}\right)(c_+(z) + c_-(z))dV$, where $c_\pm(z)$ is the *local* ion concentration and $\kappa^{-1}(z) \equiv \kappa^{-1}(c_\pm(z), \varepsilon(\Phi(z)))$ the *local* Debye length. For ions of radius $a \approx 10^{-8}$ cm and local ion concentration 10^{-3} M we find $\kappa(z) \approx 10^{-2}$ in water and at room temperature, rising to $\approx 10^{-1}$ for ion concentrations of the order of 10^{-1} M. Since the Born energy is not appreciably affected by the $\kappa(z)a$ term, we may replace to a good approximation $\kappa(z) \approx \bar{\kappa}$. Combining together the two energy terms above one finds

$$E_{\mathrm{INT}} = \chi kT \frac{1}{a^3}\int_V \Phi(z)(1-\Phi(z))dV - \frac{Z^2e^2}{2a(1+\bar{\kappa}a)}\frac{1}{a^3}\int_V \left(1-\frac{1}{\varepsilon(\Phi(z))}\right)(c_+(z)+c_-(z))dV \tag{4}$$

The local dielectric permittivity of the fluid contained in Eq. 4 can be described to a good approximation as the weighted average of solvent, ϵ_s, and polymer, ϵ_p, permittivities

$$\varepsilon(\Phi(z)) \approx \varepsilon_s(1-\Phi(z)) + \varepsilon_p\Phi(z) \tag{5}$$

a formula experimentally checked for many fluid mixtures including polymer solutions [19, 20].

The solution–solute interfacial energy per unit area $\gamma_S \equiv \gamma_S(\Phi(z))$ describes the localised energy gain (or loss) consequent to the formation of an interface. With the term *localised* we refer to distances of the order of the monomer size a. In the case of simple fluids γ_s can therefore be identified with the solvent interfacial tension. A different situation arises when polymer coils are considered; they form diffuse interfaces where the polymer concentration slowly varies over lengths much larger than the monomeric size. In that case the interfacial energy contains additional non-local terms described by Eq. 3

$$E_{\mathrm{SURF}} \approx \frac{1}{a^3}\int_V \left(\gamma_S|_{\bar{\Phi}=0} + \left.\frac{\partial\gamma_S}{\partial\bar{\Phi}}\right|_{\bar{\Phi}=0}\Phi(z)\right)h(z-a)dV \tag{6}$$

where $\gamma_S|_{\bar{\Phi}=0}$ is the interfacial energy per unit surface of pure solvent ($\bar{\Phi}=0$) while the second term measures its variation with the surface polymer concentration ($\partial\gamma_S/\partial\bar{\Phi}<0$ for polymer-adsorbing walls and $\partial\gamma_S/\partial\bar{\Phi}>0$ for repulsive walls). The local nature of these forces has been imposed through a step function $h(z-a)$ (defined as $h(z-a)=1$ for $0<z<a$ and $h(z-a)=0$ otherwise) which limits the range of the interfacial forces to a distance $z=a$ from the interface. It is worth mentioning that $\partial\gamma_S/\partial\bar{\Phi}$ does not measure the polymer–solute forces; even in the absence of direct forces (e.g. at the air–polymer solution interface) $\partial\gamma_S/\partial\bar{\Phi}$ generally differs from zero.

Finally, the energy of interaction between the solute charge distribution and the still unknown induced electrostatic potential $\psi(z)$ is

$$E_{\mathrm{INT}} = \sigma\frac{1}{a^2}\int_S \psi(z)|_{z=0}dS + Ze\frac{1}{a^3}\int_V (c_+(z)-c_-(z))\psi(z)dV \tag{7}$$

The first term describes the interaction between the solute surface charge density σ, uniformly distributed over a surface S, and the electrostatic potential generated by the surface charges. The second integral term accounts for the interaction between the ion distribution in the bulk solution and the previously defined potential.

Adding together the above energy contributions one obtains

$$\begin{aligned}\frac{E_{\mathrm{TOT}}}{kT} = {} & \frac{1}{kT}\frac{1}{a^2}\int_S \sigma.\psi(z)|_{z=0}dS \\ & + \frac{1}{a^3}\int_V [\frac{1}{kT}(\gamma_S|_{\Phi.=0} + .\frac{\partial\gamma_S}{\partial\bar{\Phi}}|_{\Phi.=0}\Phi(z))h(z-a) \\ & + \frac{a^2}{24\Phi(z)(1-\Phi(z))}(\frac{\partial\Phi(z)}{\partial z})^2 \\ & + \frac{\Phi(z)}{N}\log\frac{\Phi(z)}{N} + (1-\Phi(z))\log(1-\Phi(z)) + \chi\Phi(z)(1-\Phi(z)) \\ & + c_+(z)\log c_+(z) + c_-(z)\log c_-(z) - 2\bar{c}\log\bar{c} \\ & + \frac{Ze}{kT}(c_+(z)-c_-(z))\psi(z) - B(c_+(z)+c_-(z))(1-\frac{1}{\varepsilon(\Phi(z))})]dV\end{aligned} \tag{8}$$

where $B \equiv \frac{Z^2e^2}{2akT}\frac{1}{1+\kappa a}$. In the semi-dilute regime, $\Phi(z)<<1$, we may expand the local polymer free energy up to $O(\Phi^3(z))$

$$\frac{\Phi(z)}{N}\log\frac{\Phi(z)}{N} + (1-\Phi(z))\log(1-\Phi(z)) + \chi\Phi(z)(1-\Phi(z)) \approx \text{linear terms in } \Phi(z) + \frac{\Phi(z)}{N}\log\Phi(z) + \frac{1}{2}v\Phi^2(z) + ... \tag{9}$$

where $v \equiv 1-2\chi$ ($v>0$ means a stable homogeneous solution, when $v<0$ a polymer–solvent phase separation occurs [15]). Linear terms in $\Phi(z)$ disappear in the following mathematical handling, therefore they have not been retained.

It is worth noting that for long polymer chains, $N>>1$, the logarithmic term in Eq. 9 is negligible. On the contrary, for small molecules, $N\approx1$, the logarithmic term dominates because $\Phi(z)<<1$. These results highlight the opposite behaviour of monomeric and polymeric solvents related to the sharp decrease of mixing entropy with connectivity.

By using Eq. 9, one may rewrite the free energy functional (Eq. 8) as the *excess* free energy with respect to the bulk-phase energy due to the charged interface

$$\begin{aligned}\frac{E_{\mathrm{TOT}}}{kT} = {} & \frac{E_{\mathrm{TOT}}}{kT}|_{z\to\infty} + \frac{1}{kT}\frac{1}{a^2}\int_S \sigma\psi(z)|_{z=0}dS \\ & + \frac{1}{a^3}\int_V [\frac{1}{kT}(\gamma_S|_{\Phi_-=0} + \frac{\partial\gamma_S}{\partial\bar{\Phi}}|_{\bar{\Phi}=0}\Phi(z))h(z-a) \\ & + \frac{a^2}{24\Phi(z)}(\frac{\partial\Phi(z)}{\partial z})^2 + \frac{1}{2}v(\Phi^2(z)-\bar{\Phi}^2) \\ & + c_+(z)\log c_+(z) + c_-(z)\log c_-(z) - 2\bar{c}\log\bar{c} \\ & + \frac{Ze}{kT}(c_+(z)-c_-(z))\psi(z) - B(c_+(z) \\ & + c_-(z))(\frac{1}{\bar{\varepsilon}} - \frac{1}{\varepsilon(\Phi(z))})]dV\end{aligned} \tag{10}$$

where $\bar{\varepsilon} \equiv \varepsilon(\bar{\Phi})$ is the bulk dielectric permittivity of the polymer solution. The interesting property of the

transformed functional (Eq. 10) is that the integrand of the volume integral vanishes in the limit $z \to \infty$.

Minimisation procedure

In order to calculate the concentration profile of polymer and ions near the charged interface, one must first minimise the free energy functional given by Eq. 10.

Energy minimisation must satisfy both mass conservation and electroneutrality constraints

$$Ze\int_V (c_+(z) - c_-(z))dV = -\sigma S \tag{11a}$$

$$\int_V \Phi(z)dV = \bar{\Phi}V \tag{11b}$$

where $V \to \infty^3$ and $S \to \infty^2$ are the volume and the interface of the polymer-containing electrolyte solution, while σ is the interfacial electrical density of solute.

In order to simplify the following mathematical handling, it is useful to perform a change of variable

$$\Phi(z) = \theta^2(z) \tag{12}$$

which eliminates in Eq. 10 the disturbing $\Phi(z)$ dependence of the square gradient coefficient. Moreover, it is also convenient to partition the volume integration in two different regions: the first in the range $0 < z < a$ describes the fluid layer in direct contact with the surface; the latter, in the range $z > a$, describes the true fluid solution. Since the interface layer is narrow ($z \approx a$), we may assume as constant both the interfacial polymer concentration and the electrostatic potential

$$\theta(z)|_{z=0} = \theta(z)|_{z=a} = \text{const}, \quad \psi(z)|_{z=0} = \psi(z)|_{z=a} = \text{const} \tag{13}$$

Hence, by exploiting the integral identities $\int_V \left(\frac{\partial\theta(z)}{\partial z}\right)^2 dV = 0$ for $0 < z < a$, and $\int_V \left(\frac{\partial\theta(z)}{\partial z}\right)^2 dV = a\int_S \theta(z)\frac{\partial\theta(z)}{\partial z}\Big|_a^\infty dS - \int_V \theta(z)\frac{\partial^2\theta(z)}{\partial z^2}dV$ for $z > a$, the transformed energy functional becomes

$$\begin{aligned}\frac{E_{\mathrm{TOT}}}{kT} &= \frac{E_{\mathrm{TOT}}}{kT}|_{z\to\infty} + \frac{1}{a^2}\int_S [\frac{1}{kT}\sigma\psi(z)|_{z=a} \\ &+ \frac{1}{kT}(\gamma_{\mathrm{S}}|_{\bar{\Phi}=0} + \frac{\partial\gamma_{\mathrm{S}}}{\partial\bar{\Phi}}|_{\bar{\Phi}=0}\theta^2(z)|_{z=a}) \\ &+ Q(\theta(z), c_\pm(z), \psi(z))_{z=a} - \frac{a}{6}\theta(z)|_{z=a}\cdot\frac{\partial\theta(z)}{\partial z}|_{z=a}]dS \\ &+ \frac{1}{a^3}\int_V [-\frac{a^2}{6}\theta(z)\frac{\partial^2\theta(z)}{\partial z^2} + Q(\theta(z), c_\pm(z), \psi(z))]dV\end{aligned} \tag{14}$$

where the shorthand notation has been used:

$$\begin{aligned}Q(\theta(z), c_\pm(z), \psi(z)) \equiv &\frac{1}{2}v(\theta^4(z) - \bar{\Phi}^2 + c_+(z)\log c_+(z) \\ &+ c_-(z)\log c_-(z) - 2\bar{c}\log\bar{c}) + \frac{Ze}{kT}(c_+(z) \\ &- c_-(z))\psi(z) - B(c_+(z) + c_-(z))(\frac{1}{\bar{\varepsilon}} - \frac{1}{\varepsilon(\theta(z))})\end{aligned} \tag{15}$$

When expressed as a function of the new variable $\theta(z)$ the polymer mass conservation constraint (Eq. 11b) in the region $z > a$ becomes

$$\frac{1}{a^3}\int_V \theta^2(z)dV = \bar{\Phi}\frac{V}{a^3} - \Phi(z)|_{z=a}\frac{S}{a^2} \tag{16}$$

In this range the minimisation procedure with respect to the functions $y_j(z)$ (where $y_j(z)$ stands for $c_+(z)$, $c_-(z)$ and $\theta(z)$) under the constraints of Eqs. 11a and Eq. 11b requires the definition of a new functional

$$H = \frac{1}{kT}E_{\mathrm{TOT}} + \lambda_+ c_+(z) + \lambda_- c_-(z) + \lambda_\Phi\theta^2(z) \tag{17}$$

λ_+, λ_- and λ_Φ being three Lagrange multipliers to be determined. Extremisation of the functional (Eq. 17) is obtained by the Euler–Lagrange equation [21], $\int_V (\delta H/\delta y_j)dV = 0$, thus

$$\begin{aligned}\frac{\delta H}{\delta y_j(z)} \equiv &\frac{\partial H}{\partial y_j(z)} - \frac{\partial}{\partial z}\frac{\partial H}{\partial(\partial y_j(z)/\partial z)} + \frac{\partial^2}{\partial z^2}\frac{\partial H}{\partial(\partial^2 y_j(z)/\partial z^2)} \\ &= 0\end{aligned} \tag{18}$$

When applied to the ion concentrations the corresponding Euler–Lagrange [21] equation takes the simple form $\frac{\partial H}{\partial c_+(z)} = 0$ and $\frac{\partial H}{\partial c_-(z)} = 0$, hence

$$\log c_+(z) + 1 + \frac{Ze}{kT}\psi(z) - B\left(\frac{1}{\bar{\varepsilon}} - \frac{1}{\varepsilon(\theta(z))}\right) + \lambda_+ = 0 \tag{19a}$$

$$\log c_-(z) + 1 - \frac{Ze}{kT}\psi(z) - B\left(\frac{1}{\bar{\varepsilon}} - \frac{1}{\varepsilon(\theta(z))}\right) + \lambda_- = 0 \tag{19b}$$

The unknown Lagrange multipliers λ_+ and λ_- can be eliminated by calculating the limiting expressions to Eqs. 19a and 19b for $z \to \infty$. Since $\lim_{z\to\infty}\psi(z) = 0$, $\lim_{z\to\infty}\theta^2(z) = \bar{\Phi}$ and $\lim_{z\to\infty}c_\pm(z) = \bar{c}$, we obtain

$$c_\pm(z) = \bar{c}\exp\left(B\left(\frac{1}{\bar{\varepsilon}} - \frac{1}{\varepsilon(\theta(z))}\right)\right)\exp\left(\mp\frac{Ze\psi(z)}{kT}\right) \tag{20}$$

When $\varepsilon(\theta(z)) \to \bar{\varepsilon}$ (homogeneous polymer distribution), Eq. 20 reduces to the classical Boltzmann formula for dilute electrolyte solutions [22].

We use now the Euler–Lagrange equation to minimise the energy functional with respect to the polymer profile $\theta(z)$ yielding

$$\frac{1}{kT}\frac{\partial\gamma_S}{\partial\bar{\Phi}}|_{\Phi}\theta(z)|_{z=a}-\frac{a}{12}\frac{\partial\theta(z)}{\partial z}|_{z=a}+v\theta^3(z)|_{z=a}-\frac{1}{2}B(c_+(z)|_{z=a}+c_-(z)|_{z=a})\frac{1}{\varepsilon^2(\theta(z))}\frac{\partial\varepsilon(\theta(z))}{\partial\theta(z)}|_{z=a}=0 \tag{21a}$$

for $0<z<a$

$$\frac{a^2}{6}\frac{\partial^2\theta(z)}{\partial z^2}-\lambda_\Phi\theta(z)-v\theta^3(z)+\frac{1}{2}B(c_+(z)+c_-(z))\frac{1}{\varepsilon^2(\theta(z))}\frac{\partial\varepsilon(\theta(z))}{\partial\theta(z)}=0 \tag{21b}$$

for $z>a$.

λ_Φ being a Lagrange multiplier. Far from the solute surface, $z\to\infty$, the polymer bulk concentration is constant, thus $\theta(z)\to\bar{\Phi}^{1/2}$ and $\partial^2\theta(z)/\partial z^2\to 0$. Moreover, $c_\pm(z)\to\bar{c}$ and $\frac{1}{\varepsilon^2(\theta(z))}\frac{\partial\varepsilon(\theta(z))}{\partial\theta(z)}\to\frac{2}{\bar{\varepsilon}^2}(\varepsilon_p-\varepsilon_s)\bar{\Phi}^{1/2}$ (see Eq. 5 for the definition of $\epsilon(z)$). λ_Φ can therefore be immediately calculated

$$\lambda_\Phi=-v\bar{\Phi}+2B\frac{\varepsilon_p-\varepsilon_s}{\bar{\varepsilon}^2}\bar{c} \tag{22}$$

The knowledge of λ_Φ, together with the analytical expressions for $c_+(z)$ and $c_-(z)$ reported in Eq. 20, allows one to rewrite Eq. 21b as

$$\frac{\partial^2\hat{\theta}(z)}{\partial z^2}+2\xi^{-2}\hat{\theta}(z)\left(1-\hat{\theta}^2-D\left(1-F\left(\hat{\theta}\right)\cosh\left(\frac{Ze\psi(z)}{kT}\right)\right)\right)=0 \tag{23}$$

where $\hat{\theta}(z)\equiv\theta(z)\bar{\Phi}^{-1/2}$ and $\xi\equiv a/(3v\bar{\Phi})^{1/2}$ is the so-called Edwards correlation length [15], which is a measure of the polymer profile decay. Moreover we defined $D\equiv 6\xi^2B\frac{\varepsilon_p-\varepsilon_s}{\bar{\varepsilon}^2a^2}\bar{c}$ and $F\left(\hat{\theta}(z)\right)\equiv\left(\frac{\bar{\varepsilon}}{\varepsilon\left(\hat{\theta}(z)\right)}\right)^2\exp\left(B\left(\frac{1}{\bar{\varepsilon}}-\frac{1}{\varepsilon\left(\hat{\theta}(z)\right)}\right)\right)\approx 1+\left(\frac{B}{\bar{\varepsilon}}-2\right)\frac{\varepsilon_p-\varepsilon_s}{\bar{\varepsilon}}\bar{\Phi}\left(\hat{\theta}^2(z)-1\right)+\ldots$.

Equation 23 describes the scaled polymer profile $\hat{\theta}(z)$ near the interface under the effect of an electrolyte distribution modulated by the still unknown electrostatic potential $\psi(z)$.

Finally, minimisation of the total energy with respect to the interfacial polymer concentration $\theta(z)|_{z=a}$, Eq. 21a, provides the proper boundary condition at $z=a$ to Eq. 23. Using the analytical expressions for $c_\pm(z)|_{z=a}$ and rearranging, we get

$$\frac{\partial\hat{\theta}(z)}{\partial z}|_{z=a}=[K_1+K_2\hat{\theta}^2(z)|_{z=a}-K_3(1-A(\hat{\theta}^2(z)|_{z=a}-1))\cosh(\frac{Ze\psi(z)|_{z=a}}{kT})]\hat{\theta}(z)|_{z=a} \tag{24}$$

where $K_1\equiv\frac{12}{akT}\cdot\frac{\partial\gamma_S}{\partial\Phi}\Big|_{\bar{\Phi}=0}$, $K_2\equiv 12\frac{v}{a}\bar{\Phi}$, $K_3\equiv 24\frac{B}{a\varepsilon}\frac{\varepsilon_p-\varepsilon_s}{\bar{\varepsilon}}\bar{c}$ and $A\equiv\frac{B}{\bar{\varepsilon}}\left(\frac{B}{\bar{\varepsilon}}-2\right)\frac{\varepsilon_p-\varepsilon_s}{\bar{\varepsilon}}\bar{\Phi}$.In the absence of ions ($\bar{c}=0$) we recover from Eqs. 23 and 24 the celebrated de Gennes equation and boundary condition for polymers at an interface [15].

The last unknown function to be determined is the electrostatic potential inside the polymer-containing electrolyte solution. The electrostatic potential $\psi(z)$ must satisfy the Poisson equation [23]: $div(\varepsilon(\vec{r})\nabla\psi(\vec{r}))=-4\pi\rho(\vec{r})$, where $\rho(\vec{r})$ is the density of the free moving charges dispersed in the dielectric medium: $\rho(\vec{r})=\rho(z)=Ze(c_+(z)-c_-(z))$. With the aid of Eqs. 5 and 20, which provide the analytical expressions of the electrolyte concentration $c_\pm(z)$ and dielectric permittivity profile $\varepsilon\left(\hat{\theta}(z)\right)$, the Poisson equation takes the following form

$$\frac{\partial}{\partial z}(\varepsilon(\hat{\theta}(z))\frac{\partial\psi(z)}{\partial z})=\frac{\bar{\varepsilon}kT}{Ze}\bar{\kappa}^2\cdot\exp\left(B(\frac{1}{\bar{\varepsilon}}-\frac{1}{\varepsilon(\hat{\theta}(z))})\right)\sinh(\frac{Ze\psi(z)}{kT}) \tag{25}$$

where $\bar{\kappa}^{-1}\equiv\left(\frac{8\pi Z^2e^2\bar{c}}{\bar{\varepsilon}kT}\right)^{-1/2}$ is the bulk Debye length, a measure of the electrostatic potential decay inside an electrolyte solution [22]. The coupling between the electrostatic potential $\psi(z)$ and the polymer concentration profile $\hat{\theta}(z)$is evident from Eq. 25. This equationmust satisfy the obvious boundary conditions at infinity

$$\lim_{z\to\infty}\psi(z)=0 \tag{26}$$

The boundary condition at the solute–solvent interface $z=0$ can be obtained by integrating the Poisson equation (Eq. 25) over the whole solvent volume V. By invoking the electroneutrality condition (Eq. 11a) we obtain

$$\varepsilon\left(\hat{\theta}(z)\Big|_{z=0}\right)\cdot\frac{\partial\psi(z)}{\partial z}\Big|_{z=0}=-4\pi Ze\frac{1}{S}\int_V(c_+(z)-c_-(z))dV=4\pi\sigma \tag{27}$$

where σ is the solute surface charge density.

Calculation of the polymer and electrolyte profiles

Equations 23 and 25 are the main result of this paper. They describe two coupled non-linear differential equations (NLDE) satisfying non-trivial boundary conditions at the solute–solvent interface, Eqs. 24 and 27,

together with the obvious limits $\lim_{z\to\infty}\hat{\theta}(z)=1$ and $\lim_{z\to\infty}\psi(z)=0$. Their analytical structure somewhat resembles that of the coupled exciton–soliton motion [24]; this interesting analogy, however, will not pursued here. Although only numerical solutions can be obtained to our equations, asymptotic solutions can be calculated analytically in all but a few interesting cases. In the following we list some useful limits to the NLDE system.

Small surface charge density and weak polymer adsorption

In the case of small surface charge density σ of the solute surface the electrostatic potential $\psi(z)$ is small everywhere, namely one may approximate $\sinh\left(\frac{Ze\psi(z)}{kT}\right)\approx\frac{Ze}{kT}\psi(z)$ and $\cosh\left(\frac{Ze\psi(z)}{kT}\right)\approx 1+O\left(\left(\frac{Ze\psi(z)}{kT}\right)^2\right)$. The polymer concentration profile is ruled by Eq. 23 which, for small $\psi(z)$, yields a simple equation

$$\frac{\partial^2\hat{\theta}(z)}{\partial z^2}-2\xi_{\mathrm{eff}}^{-2}\hat{\theta}(z)\left(1-\hat{\theta}^2(z)\right)=0 \tag{28}$$

where $\xi_{\mathrm{eff}}^{-2}\equiv\xi^{-2}-6a^{-2}\frac{B}{\bar{\varepsilon}}\left(\frac{B}{\bar{\varepsilon}}-2\right)\left(\frac{\varepsilon_p-\varepsilon_s}{\bar{\varepsilon}}\right)^2\bar{c}\bar{\Phi}$. It is worth noting that, even to the lowest approximation ($\psi(z)\to 0$), the model predicts a coupling between polymer and electrolyte concentration. The main effect is a re-normalisation of the decay lengths of the polymer profile ξ_{eff}. The solution to Eq. 28 satisfying the boundary condition $\lim_{z\to\infty}\hat{\theta}(z)=1$ is analytical,

$$\hat{\theta}(z) = \begin{matrix} ctgh\left(\frac{z+z_o}{\xi_{\mathrm{eff}}}\right) \\ tgh\left(\frac{z+z_o}{\xi_{\mathrm{eff}}}\right) \end{matrix} \tag{29}$$

the upper formula being valid for polymer adsorbing interfaces while the lower one applies for repelling interfaces. z_o is an integration constant to be determined by applying the boundary condition (Eq. 24) and ξ_{eff} is the salt-modified Edwards correlation length. Inserting the analytical expression for $\hat{\theta}(z)$ into Eq. 24 and using the identity [25] $1=ctgh^2x-1/(\sinh^2x)$, we find an implicit expression for the integration constant z_o

$$S_1f^3+f^2+S_2f-1=0 \tag{30}$$

where $f\equiv ctgh\left(\frac{z_o}{\xi_{\mathrm{eff}}}\right)\equiv\left(\Phi(z)|_{z=0}/\bar{\Phi}\right)^{1/2}$ is the scaled interfacial polymer concentration and $S_1\equiv\xi_{\mathrm{eff}}(K_1-K_3(1+A))$; $S_2\equiv\xi_{\mathrm{eff}}(K_2+K_3A)$.

Once the analytical expression for the polymer concentration $\Phi(z)=\bar{\Phi}\hat{\theta}^2(z)$ has been obtained, we proceed further by calculating the polymer-modified profile of the ion concentration. This task can be performed only if the electrostatic potential $\psi(z)$ is known. This can be calculated from the linearised Poisson–Boltzmann equation (Eq. 25) performing first the change of variable $\psi(z)=S(z)/\sqrt{\varepsilon\left(\hat{\theta}(z)\right)}$ which transforms Eq. 25 into

$$\begin{aligned}&\frac{\partial^2S(z)}{\partial z^2}-\frac{1}{\varepsilon(\hat{\theta}(z))}\left[\bar{\varepsilon}\bar{\kappa}^2\cdot\exp\left(B\left(\frac{1}{\bar{\varepsilon}}-\frac{1}{\varepsilon(\hat{\theta}(z))}\right)\right)\right.\\&\left.+\frac{\partial^2\varepsilon(\hat{\theta}(z))}{\partial z^2}-\frac{1}{2\varepsilon(\hat{\theta}(z))}\left(\frac{\partial\varepsilon(\hat{\theta}(z))}{\partial z}\right)^2\right]S(z)\\&\approx\frac{\partial^2S(z)}{\partial z^2}-\left(\bar{\kappa}^2+C_2\exp\left(-\frac{2}{\xi_{\mathrm{eff}}}(z+z_o)\right)\right)S(z)\\&=0\end{aligned} \tag{31}$$

with $C_2\equiv\left(\frac{B}{\bar{\varepsilon}}-1\right)\frac{\varepsilon_p-\varepsilon_s}{\bar{\varepsilon}}\bar{\Phi}\bar{\kappa}^2-\frac{8}{\bar{\varepsilon}}\xi_{\mathrm{eff}}^{-2}$, since for polymers adsorbing at the interface $\epsilon_p<\epsilon_s$, hence $C_2<0$. In deriving Eq. 31 we related the dielectric permittivity and polymer concentration by Eq. 5 and used the analytical expression for the polymer profile previously obtained. The last approximate form of Eq. 31 is valid only in the weak adsorption limit. In that case the constant z_o is large (it logarithmically diverges when the scaled polymer surface adsorption energy goes to zero). This observation allowed us to use in deriving Eq. 31 the expansion [25] $ctgh\left(\frac{z+z_o}{\xi_{\mathrm{eff}}}\right)\approx 1+2\cdot\exp\left(-\frac{2}{\xi_{\mathrm{eff}}}(z+z_o)\right)+\ldots$. The further change of variable $\exp\left(-\frac{2}{\xi_{\mathrm{eff}}}(z+z_o)\right)=\frac{y^2}{|C_2|\xi_{\mathrm{eff}}^2}$ transforms Eq. 31 into an ordinary Bessel differential equation

$$\frac{\partial^2S(y)}{\partial y^2}+\frac{1}{y}\frac{\partial S(y)}{\partial y}+\left(1-\frac{\mu^2}{y^2}\right)S(y)=0 \tag{32}$$

(with $\mu\equiv\bar{\kappa}\xi_{\mathrm{eff}}$) whose general solution is [26]

$$S(y)=A_1J_\mu(y)+A_2Y_\mu(y) \tag{33}$$

A_1 and A_2 being two integration constants to be determined while $J_\mu(y)$ and $Y_\mu(y)$ are two linearly independent solutions to Eq. 32. Recalling that $\lim_{y\to 0}y=0$ and $\lim_{y\to 0}Y_\mu(y)\to\infty$, it follows that $A_2=0$. Because of the relationship $\psi(z)=S(z)/\sqrt{\varepsilon\left(\hat{\theta}(z)\right)}$, the remaining integration constant, A_1, can be easily obtained through the boundary condition (Eq. 27). Simple algebra yields

$$A_1=\frac{4\pi\sigma}{-\frac{1}{2}\varepsilon^{-1/2}\left(\hat{\theta}(z)\right)\frac{\partial\varepsilon(\hat{\theta}(z))}{\partial z}J_\mu(y)|_{z=0}+\varepsilon^{1/2}\left(\hat{\theta}(z)\right)\frac{\partial J_\mu(y)}{\partial z}\Big|_{z=0}} \tag{34}$$

In the weak absorption limit $y<<1$, hence [25] $J_\mu(y)\approx\left(\frac{1}{2}y\right)^\mu\frac{1}{\Gamma(\mu+1)}+O\left(y^{\mu+2}\right)$ ($\Gamma(x)$ being the gamma function). Combining the above results, the interfacial electrostatic potential $\psi(z)|_{z=0}$ reads

$$\psi(z)|_{z=0}\approx\frac{4\pi\sigma}{\bar{\kappa}\varepsilon\left(\hat{\theta}(z)\right)\Big|_{z=0}+\frac{1}{2}\frac{\partial\varepsilon(\hat{\theta}(z))}{\partial z}\Big|_{z=0}} \tag{35}$$

a simple formula that for constant dielectric permittivity ($\varepsilon(\hat{\theta}(z))=\bar{\varepsilon}$) reduces to the well-known result $\psi(z)|_{z=0}=$

$\frac{4\pi\sigma}{\bar{\varepsilon}\bar{\kappa}}$ [22]. We may easily calculate the denominator of Eq. 35 obtaining to the leading terms

$$\psi(z)|_{z=0} \approx \frac{4\pi\sigma}{\bar{\varepsilon}\bar{\kappa}}\left[1+\left(\frac{1}{2}\left(\frac{B}{\bar{\varepsilon}}+1\right)-\frac{1}{\bar{\kappa}\xi_{\mathrm{eff}}}\right)\frac{\varepsilon_{\mathrm{p}}-\varepsilon_{\mathrm{s}}}{\bar{\varepsilon}}\bar{\Phi}\xi_{\mathrm{eff}}K_{\mathrm{eff}}\right] \tag{36}$$

where $K_{\mathrm{eff}}<0$ is the effective surface polymer energy $K_{\mathrm{eff}}\equiv\frac{12}{a}\left(\frac{1}{kT}\frac{\partial\gamma_{\mathrm{s}}}{\partial\Phi_{-}}\Big|_{\bar{\Phi}=0}+\nu\bar{\Phi}-2\frac{B}{\bar{\varepsilon}}\frac{\varepsilon_{\mathrm{p}}-\varepsilon_{\mathrm{s}}}{\bar{\varepsilon}}\bar{c}\right)$. Since in general $\epsilon_{\mathrm{p}}-\epsilon_{\mathrm{s}}<0$ for polymers adsorbing at the interface and $1/\bar{\kappa}\xi_{\mathrm{eff}}<<B/\bar{\varepsilon}$, it follows that the term in the square brackets is greater than 1.

Introducing the equations for the polymer concentration $\hat{\theta}(z)$ and electrostatic potential $\psi(z)$ into the expression for $c_{\pm}(z)$, eventually one finds a simple expression for the interfacial ion concentration

$$c_{\pm}(z)|_{z=0}\approx\bar{c}\left[1-\frac{B}{\bar{\varepsilon}}\frac{\varepsilon_{\mathrm{p}}-\varepsilon_{\mathrm{s}}}{\bar{\varepsilon}}\bar{\Phi}|K_{\mathrm{eff}}\xi_{\mathrm{eff}}|\mp\frac{Ze}{kT}\psi(z)|_{z=0}\right] \tag{37}$$

while the surface polymer concentration is simply

$$\Phi(z)|_{z=0}=\bar{\Phi}(1-|K_{\mathrm{eff}}\xi_{\mathrm{eff}}|) \tag{38}$$

These simple equations (Eqs. 37 and 38) are noticeable and will be discussed later.

High electrolyte concentration

When the salt concentration is rather high, the decay of the electrostatic potential on going from the charged interface to the interior of the electrolyte solution is much faster than that of polymer concentration. More precisely, this condition is fulfilled when the Debye length $1/\bar{\kappa}$ is far larger than the Edwards correlation length ξ, namely $\frac{8\pi Z^2e^2\bar{c}}{\bar{\varepsilon}kT}>>\frac{3\nu\bar{\Phi}}{a^2}$. Under the above condition the local dielectric permittivity $\varepsilon(\Phi(z))$ remains essentially constant in the range of the electrostatic potential variation allowing us to approximate $\varepsilon\left(\hat{\theta}(z)\right)\approx\varepsilon\left(\hat{\theta}(z)|_{z=0}\right)$. The modified Poisson–Boltzmann equation (Eq. 25) becomes

$$\frac{\partial^2\psi(z)}{\partial z^2}-\frac{kT}{Ze}\kappa_{\mathrm{eff}}^2\cdot\sinh\left(\frac{Ze\psi(z)}{kT}\right)=0 \tag{39}$$

where $\kappa_{\mathrm{eff}}^2\equiv\bar{\kappa}^2\frac{\bar{\varepsilon}}{\varepsilon(\hat{\theta}(z)|_{z=0})}\exp\left(B\left(\frac{1}{\bar{\varepsilon}}-\frac{1}{\varepsilon(\hat{\theta}(z)|_{z=0})}\right)\right)$. The solution to Eq. 39 is analytical [22]

$$\psi(z)=\frac{2kT}{Ze}\log\frac{1+\Gamma e^{-\kappa_{\mathrm{eff}}z}}{1-\Gamma e^{-\kappa_{\mathrm{eff}}z}} \tag{40}$$

where $\Gamma\equiv tgh\left(Ze\psi(z)|_{z=0}/4kT\right)$. By applying the boundary condition at the interface (Eq. 27) one obtains $\frac{kT}{Ze}\varepsilon\left(\hat{\theta}(z)\right)|_{z=0}\kappa_{\mathrm{eff}}\Gamma\left(1-\Gamma^2\right)^{-1}=\pi\sigma$, from which the searched relationship between surface charge density σ and surface electrostatic potential $\psi(z)|_{z=0}$ is easily found:

$$\psi(z)|_{z=0}\approx\begin{cases}\dfrac{4\pi\sigma}{\varepsilon\left(\hat{\theta}(z)\right)|_{z=0}\kappa_{\mathrm{eff}}} & \sigma\ \text{Small}\\ \dfrac{2kT}{Ze}\log\dfrac{Ze}{kT}\dfrac{4\pi\sigma}{\varepsilon\left(\hat{\theta}(z)\right)|_{z=0}\kappa_{\mathrm{eff}}} & \sigma\ \text{Large}\end{cases} \tag{41}$$

The polymer concentration is modified by the electrolyte concentration just inside a thin layer near the charged surface. Within this layer (whose thickness is of the order $1/\bar{\kappa}$) the potential drops from $\psi(z)|_{z=0}$ to nearly zero, while the polymer concentration remains fairly constant about the interfacial value $\approx\bar{\Phi}\hat{\theta}^2(z)|_{z=0}$. Outside the boundary layer the potential $\psi(z)$ is practically zero while the polymer concentration slowly decays towards the bulk value $\bar{\Phi}$. The above reasoning suggests we should adopt a simple interpolating expression for the electrostatic potential

$$\psi(z)\approx\begin{cases}\psi(z)|_{z=0}-\left|\dfrac{\partial\psi(z)}{\partial z}\Big|_{z=0}\right|\cdot z & 0<z<0_{\mathrm{crit}}\\ 0 & z>z_{\mathrm{crit}}\end{cases} \tag{42}$$

where z_{crit} is the distance at which the potential vanishes $z_{\mathrm{crit}}\approx\frac{\psi(z)|_{z=0}}{\left|\frac{\partial\psi(z)}{\partial z}\right|_{z=0}}$, while analytical expressions for $\psi(z)|_{z=0}$ and $\partial\psi(z)/\partial z|_{z=0}$ are given by Eqs. 27 and 41. After replacing the approximate expression for $\psi(z)$ into the free energy functional (Eq. 10) and minimising by the Euler–Lagrange equation in the outer region $z>z_{\mathrm{crit}}$, we find

$$\frac{\partial^2\hat{\theta}(z)}{\partial z^2}+2\xi_{\mathrm{eff}}^{-2}\hat{\theta}(z)\left(1-\hat{\theta}^2(z)\right)=0 \tag{43}$$

an equation which is independent of $\psi(z)$. Minimisation of the free energy functional inside the interfacial layer $0<z<z_{\mathrm{crit}}$, together with the condition of constant polymer concentration within the layer $\theta(z)|_{z=z_{\mathrm{crit}}}\approx\theta(z)|_{z=a}\approx\theta(z)|_{z=0}$, yields a non-linear algebraic equation which fixes the boundary condition to the differential equation (Eq. 43)

$$\frac{1}{kT}\frac{\partial\gamma_{\mathrm{s}}}{\partial\bar{\Phi}}\Big|_{\bar{\Phi}}\theta(z)|_{z=a}-\frac{a}{12}\frac{\partial\theta(z)}{\partial z}\Big|_{z=a}+\nu\theta^3(z)|_{z=a} -\frac{1}{2}B\left(\frac{1}{z_{\mathrm{crit}}}\int_0^{z_{\mathrm{crit}}}(c_+(z)+c_-(z))dz\right)\frac{1}{\varepsilon^2(\theta(z))}\frac{\partial\varepsilon(\theta(z))}{\partial\theta(z)}\Big|_{z=a} =0 \tag{44}$$

Equation 44 is similar to that obtained in the general theory and reported by Eq. 21a, the only difference being that the interfacial electrolyte concentration $c_+(z)|_{z=a}+c_-(z)|_{z=a}$ is now replaced by the mean electrolyte concentration $\left(\frac{1}{z_{\mathrm{crit}}}\int_0^{z_{\mathrm{crit}}}(c_+(z)+c_-(z))dz\right)$

calculated within a thin layer of thickness z_{crit}. Following the same procedure used in deriving the boundary condition (Eq. 24) we obtain

$$\frac{\partial\hat{\theta}(z)}{\partial z}|_{z=a} = [K_1 + K_2\hat{\theta}^2(z)_{z=a} - K_3(1 - A(\hat{\theta}^2.(z)|_{z=a} - 1)\frac{\sinh(\frac{Ze}{kT}\psi.(z)|_{z=a})}{\frac{Ze}{kT}\psi.(z)|_{z=a}}]\hat{\theta}.(z)|_{z=a} \quad (45)$$

which differs from Eq. 24 just for the potential-dependent term. The solution to Eq. 43 satisfying the condition $\lim_{z\to\infty}\hat{\theta}(z) = 1$ is identical to that obtained for small interface charge density as reported in Eq. 29; the boundary conditions at the interface are, however, different.

It is worth noting that at high electrolyte concentration the original coupled NLDEs can be decoupled into two independent equations, both having exact and simple analytical solutions. The coupling between polymer and electrolyte profiles is now transferred to rather complex boundary conditions given by Eqs. 27 and 45.

Let us analyse in more detail the behaviour of the interfacial polymer density in the case of high and small surface charge density σ. When the electrical density of the solute surface is small, the potential $\psi(z)|_{z=a}$ is also small. Recalling that $\frac{\sinh x}{x} \underset{x\to 0}{\to} 1 + O(x^2)$, the boundary condition (Eq. 45) becomes identical to that calculated in the previous section for weak surface density. In that case the surface potential $\psi(z)|_{z=a}$ is given by Eq. 36.

On the contrary, at high potentials we may set $\sinh x \underset{x>>1}{\to} \frac{1}{2}e^{|x|}$. By exploiting the relationship between σ and $\psi(z)|_{z=0}$ given by Eq. 41 and recalling that $\psi(z)|_{z=0} = \psi(z)|_{z=a}$, we obtain a simple equation for the interfacial potential

$$\psi(z)|_{z=a} \approx 2\frac{kT}{Ze}\log\frac{Ze}{kT}\frac{4\pi|\sigma|}{\bar{\varepsilon}\bar{\kappa}} - \frac{kT}{Ze}\left(\frac{B}{\bar{\varepsilon}}\left(1 - \frac{\bar{\varepsilon}}{\varepsilon\left(\hat{\theta}(z)|_{z=a}\right)}\right) + \log\frac{\varepsilon\left(\hat{\theta}(z)|_{z=a}\right)}{\bar{\varepsilon}}\right) \quad (46)$$

with $\varepsilon\left(\theta(z)|_{z=a}\right) \approx \varepsilon_s$, namely the dielectric permittivity of the polymer solution near the interface is roughly equal to that of pure solvent. Since $\varepsilon_s > \bar{\varepsilon}$ for adsorbing polymers, it follows that the correction to the surface potential due to inhomogeneous polymer–electrolyte solution mixing is *always* negative. It is worth recalling that at low surface charge density this correction is *always* positive. Following the same procedure used to calculate the interfacial electrolyte concentration at low solute surface charge density σ, we obtain in the limit of high σ

$$c_{\pm}(z)|_{z=0} \approx \bar{c}\frac{\bar{\varepsilon}}{\varepsilon\left(\hat{\theta}(z)|_{z=a}\right)}\left(\frac{Ze}{kT}\frac{4\pi|\sigma|}{\bar{\varepsilon}\bar{\kappa}}\right)^{\mp 2} \quad (47)$$

Again $\varepsilon\left(\theta(z)|_{z=a}\right) \approx \varepsilon_s$, while from Eq. 45 the surface polymer concentration is simply

$$\Phi(z)|_{z=a} \propto \left(\frac{\log\sigma}{\sigma}\right)^4 \underset{\sigma\to\infty}{\to} 0 \quad (48)$$

namely, polymer coils are expelled from the charged surface by the large number of adsorbed ions.

Finally, when the surface potential is high, but still comparable with the polymer adsorption energy at the solute interface, we must consider the full expression for the boundary condition given by Eq. 45. The final formula is a cubic algebraic equation identical to Eq. 30 but with different coefficients

$$S_1'f^3 + f^2 + S_2'f - 1 = 0 \quad (49)$$

where $S_1' \equiv \xi_{eff}\left(K_1 - \frac{1}{2}K_3(1+A)\frac{C^2}{\log C^2}\right)$ and $S_2' \equiv \xi_{eff}\left(K_2 + \frac{1}{2}K_3A\frac{C^2}{\log C^2}\right)$, the charge density-related C coefficient being $C \equiv \frac{Ze}{kT}\frac{4\pi\sigma}{\bar{\varepsilon}\bar{\kappa}}$. The most interesting feature of Eq. 49 is that multiple roots to f may occur. Standard analysis of the cubic equation (Eq. 49) shows that the onset of real and distinct roots arises when [25] $x(x - S_2')^3 = \left(\frac{3}{2}xS_2' + \frac{3}{2} - x^3\right)^2$, with $x \equiv \frac{1}{3S_1'}$. Such an identity takes place only for $S_2' >> S_1'$ (more exactly when $S_1' \approx \frac{1}{\sqrt{3+\frac{3}{4}S_2'}}$). From a physical point of view this happens when polymer adsorption is roughly compensated by the interfacial polymer expulsion consequent to the potential-induced ion gathering at the charged interface.

A similar analysis has been performed for the previously described cases of very small and very high surface charge density (Eqs. 38 and 48). In both cases only a single real root has been found.

Calculation of the solvation energy

Once the concentration profile of electrolytes and polymer near the solute–solvent interface has been calculated, we proceed further to obtain an analytical expression for the solvation energy.

Replacing the analytical expressions for $\log c_+(z)$ and $\log c_-(z)$ given by Eq. 20 into the energy functional (Eq. 10) and making use of the mass conservation constraint (Eq. 11a), one may rewrite the ion mixing entropy term as

$$\frac{1}{a^3}\int_V [c_+(z)\log c_+(z) + c_-(z)\log c_-(z) - 2\bar{c}\log\bar{c}]dV = \text{const} + \frac{1}{a^3}\int_V \left[B\left(\frac{1}{\bar{\varepsilon}} - \frac{1}{\varepsilon(\theta(z))}\right)(c_+(z) + c_-(z)) - \frac{Ze\psi(z)}{kT}(c_+(z) - c_-(z))\right]dV$$

Now, inserting the above formula into Eq. 10 and rearranging, the $c_{\pm}(z)$-dependent energy contributions cancel each other while only the $\theta(z)$-dependent ones survive. Moreover, replacing also the formulas for the surface polymer density $\theta^2(z)\big|_{z=0}$ and its gradient $\partial\theta(z)/\partial z|_{z=0}$ given by Eq. 21a, eventually we obtain a simple result for the total energy

$$\frac{E_{\mathrm{TOT}}^{\mathrm{OPTIMISED}}}{kT} = \frac{E_{\mathrm{TOT}}}{kT}\Big|_{z\to\infty} + \frac{1}{kT}\frac{1}{a^2}\int_S (.\gamma_{\mathrm{S}}|_{\bar{\Phi}=0} + .\frac{\partial\gamma_{\mathrm{S}}}{\partial\bar{\Phi}}|_{\bar{\Phi}=0}.\theta^2(z)|_{z=0} + +\sigma.\psi(z)|_{z=0})dS + \frac{1}{a^3}\int_V [\frac{a^2}{6}(\frac{\partial\theta(z)}{\partial z})^2 + \frac{1}{2}v(\theta^4(z) - \bar{\Phi}^2)]dV \tag{51}$$

It is worth noting that the above energy functional depends now only on the polymer concentration $\Phi(z) = \theta^2(z)$ and *interfacial* electrostatic potential $\psi(z)|_{z=0}$ but it does not depend any longer on the *local* potential $\psi(z)$. It must be recalled, however, that the polymer concentration is in turn related to the electrostatic potential through a system of coupled NLDEs (Eqs. 23 and 25). The simple result described above is not true in general. It holds provided the $c_{\pm}(z)$-dependent part of the energy functional is of the kind $c_{\pm}(z)\log c_{\pm}(z) + F(\theta(z))\cdot c_{\pm}(z)$ (i.e. dilute electrolyte solutions where $c_{\pm}^2(z)$ terms are lacking), otherwise the minimised energy functional (Eq. 51) does also contain $\psi(z)$-dependent terms.

Small surface charge density

When the surface charge density of solute is small the electrostatic potential has a negligible effect on the polymer distribution. Even in the absence of a surface potential, the presence of free moving ions modifies the polymer distribution because of the ion–polymer partial incompatibility.

Replacing the analytical expression for $\theta(z)$ and $\psi(z)|_{z=0}$ calculated from Eqs. 29 and 35 into the minimised energy functional (Eq. 51) and integrating (all the integrals have close analytical expressions) we get the following expression for the total energy per unit surface

$$\frac{a^2}{S}\frac{E_{\mathrm{TOT}}^{\mathrm{OPTIMISED}}}{kT} = \frac{1}{kT}\sigma\psi(z)|_{z=0} + \frac{1}{kT}\gamma_{\mathrm{S}}|_{\bar{\Phi}=0} + \frac{a}{12}K_1\bar{\Phi}f^2 + \frac{a\bar{\Phi}}{18\xi_{\mathrm{eff}}}\left[2(1-2\eta) - 3(1-\eta)f + (1+\eta)f^3\right] \tag{52}$$

where $f \equiv ctgh\left(\frac{z_o}{\xi_{\mathrm{eff}}}\right) \equiv \left(\Phi(z)|_{z=0}/\bar{\Phi}\right)^{1/2} \geqslant 1$ is the scaled interfacial polymer concentration given by Eq. 30 and $\eta \equiv (\xi_{\mathrm{eff}}/\xi)^2$.

The physical meaning of the different terms is transparent. The first one describes the electrostatic interaction (per unit surface) between the solute charge density σ and the electrostatic potential related to the polymer-modified electrolyte distribution. The second term is the interfacial tension of pure solvent ($\bar{\Phi} = 0$), a value generally increased by the presence of electrolytes [27, 28, 29]. The third contribution describes the reduction of the solvent interfacial tension due to polymer adsorption at the interface ($K < 0$). Finally, the last term describes the energy of the "diffuse" interface due to the connectivity-related correlation of the polymer chains.

In the limit of weak polymer adsorption $f = 1 + \tau$ with $\tau << 1$; this allows us to expand Eqs. 30 and 52 in power series of τ. Solving for τ and combining these results with the analytical expression for $\psi(z)|_{z=0}$ given by Eq. 36, eventually we obtain to the leading terms

$$\frac{a^2}{S}\frac{E_{\mathrm{TOT}}^{\mathrm{OPTIMISED}}}{kT} \approx \frac{4\pi\sigma^2}{\bar{\varepsilon}\bar{\kappa}kT}\left[1 + \left(\frac{1}{2}\left(\frac{B}{\bar{\varepsilon}} + 1\right) - \frac{1}{\bar{\kappa}\xi_{\mathrm{eff}}}\right)\frac{\varepsilon_{\mathrm{p}} - \varepsilon_{\mathrm{s}}}{\bar{\varepsilon}}\bar{\Phi}K_{\mathrm{eff}}\right] + \frac{1}{kT}\gamma_{\mathrm{S}}|_{\bar{\Phi}=0} + \frac{a\bar{\Phi}}{6}\left[\frac{1}{2}K_1 - \left(\frac{\xi_{\mathrm{eff}}}{\xi}\right)^2 K_{\mathrm{eff}}\right] \tag{53}$$

where $\frac{4\pi\sigma^2}{\bar{\varepsilon}\bar{\kappa}kT}$ is the electrostatic energy of a flat charged surface imbedded in a homogeneous electrolyte solution (polymer enters in modifying the averaged dielectric permittivity $\bar{\varepsilon}$ and Debye length $\bar{\kappa}$). The term in the square brackets accounts for the ion redistribution associated with the polymer inhomogeneous profile near the interface ($K_1 \equiv \frac{12}{akT}\cdot\frac{\partial\gamma_{\mathrm{S}}}{\partial\bar{\Phi}}\Big|_{\bar{\Phi}=0} < 0$ is the polymer interfacial energy in the absence of electrolytes; $K_{\mathrm{eff}} \equiv K_1 + \frac{12}{a}\left(v\Phi_{\_} - 2\frac{B}{\varepsilon_{\_}}\frac{\varepsilon_{\mathrm{p}} - \varepsilon_{\mathrm{s}}}{\varepsilon_{\_}}c_{\_}\right)$ is the *effective* interfacial energy corrected for ion rearranging near the interface and for polymer–polymer repulsion). The last terms in Eq. 53 $\frac{1}{kT}\gamma_{\mathrm{S}}|_{\bar{\Phi}=0} + \frac{a\bar{\Phi}}{6}\left[\frac{1}{2}K_1 - \left(\frac{\xi_{\mathrm{eff}}}{\xi}\right)^2 K_{\mathrm{eff}}\right]$ describe the interfacial tension of the polymer solution. This is sensitive to the salt concentration which re-normalizes the decay length ξ of the polymer profile $\xi_{\mathrm{eff}}^{-2} \equiv \xi^{-2} - 6a^{-2}\frac{B}{\bar{\varepsilon}}\left(\frac{B}{\bar{\varepsilon}} - 2\right)\left(\frac{\varepsilon_{\mathrm{p}} - \varepsilon_{\mathrm{s}}}{\bar{\varepsilon}}\right)^2\bar{c}\bar{\Phi}$, while the effect of the electrostatic potential on the polymer interfacial tension is small at low σ.

In writing the final equations for the total solvation energy (Eqs. 53 and 54) we reported only the *dressed* contribution to the electrostatic potential, a positive term that depends both on the surface charge density σ and on the solution dielectric properties and ion concentration. The *bare* contribution (negative), depending only on σ, does not change on varying the solvent properties.

High electrolyte concentration

At high electrolyte concentration the equations for the electrostatic potential and polymer concentration are not restricted to the small surface charge density case, but a general expression covering the whole range of charge density σ can be obtained. For the sake of

compactness and in order to gain a better insight into the different energy contributions, we report the limiting formulas obtained for small and high σ. When σ is small the optimised total energy becomes identical to that calculated by Eq. 53. However, when σ is very large we obtained a completely different equation

$$\frac{a^2}{S}\frac{E_{\mathrm{TOT}}^{\mathrm{OPTIMISED}}}{kT} \approx 2\frac{|\sigma|}{Ze}\log\frac{Ze}{kT}\frac{4\pi|\sigma|}{\bar{\varepsilon}\bar{\kappa}} - \frac{kT}{Ze}\left(\frac{B}{\bar{\varepsilon}}\left(1-\frac{\bar{\varepsilon}}{\varepsilon(\hat{\theta}.(z)|_{z=a})}\right)\right.$$
$$\left.+\log\frac{\varepsilon(\hat{\theta}.(z)|_{z=a})}{\bar{\varepsilon}}\right)+\frac{1}{kT}\cdot\gamma_{\mathrm{S}}|_{\bar{\Phi}=0}+\frac{a^2\bar{\Phi}}{9\xi_{\mathrm{eff}}}\left(1+2\left(\frac{\xi_{\mathrm{eff}}}{\xi}\right)^2\right) \tag{54}$$

In the large σ limit $2\frac{|\sigma|}{Ze}\log\frac{Ze}{kT}\frac{4\pi|\sigma|}{\bar{\varepsilon}\bar{\kappa}}$ describes the electrostatic energy of a flat charged surface imbedded in a homogeneous electrolyte solution. The second term in Eq. 54 describes the variation of the electrostatic energy related to the inhomogeneous polymer distribution. The effect is considered through the interfacial dielectric permittivity $\varepsilon\left(\theta(z)|_{z=a}\right)$ of the polymer + electrolyte solution (at high σ values $\varepsilon\left(\theta(z)|_{z=a}\right)\approx\varepsilon$, the pure solvent dielectric permittivity). Finally, the last two terms of Eq. 54, $\frac{1}{kT}\gamma_{\mathrm{S}}|_{\bar{\Phi}=0}+\frac{a^2\bar{\Phi}}{9\xi_{\mathrm{eff}}}\left(1+2\left(\frac{\xi_{\mathrm{eff}}}{\xi}\right)^2\right)$, describe the interfacial tension $\gamma_{\mathrm{S}}(\bar{\Phi})$ of the polymer solution. Notice the different expression obtained for $\gamma_{\mathrm{S}}(\bar{\Phi})$ in the limit of small, Eq. 53, and large, Eq. 54, σ values.

The behaviour of the optimised total free energy (Eqs. 53 and 54) on varying polymer or electrolyte concentration or surface charge density will be discussed in the next section.

Results and discussion

The mean-field model here developed allows one to predict, at least qualitatively, several properties of solute–solvent interactions in mixed solvents. It is evident from the limiting cases investigated that the idea of treating a complex solvent by a weighted average (WA) of the different component properties dramatically fails in several circumstances. Considerable deviations from the WA picture naturally emerge from the present model. Furthermore, new phenomena totally lacking in a WA picture take place. In particular, three effects described below seem to be worth investigating in the future.

Properties of the polymer solution far from the solute interface

Even far from the interface salt addition strongly affects the behaviour of the polymer solution. Since far from the surface the gradient term of the free energy functional (Eq. 10) goes to zero, a standard linear stability analysis shows that phase separation in polymer-rich and electrolyte-rich phases occurs when the effective polymer decay length ξ_{eff} is greater than zero, namely $\xi^{-2}-6a^{-2}\frac{B}{\bar{\varepsilon}}\left(\frac{B}{\bar{\varepsilon}}-2\right)\left(\frac{\varepsilon_{\mathrm{p}}-\varepsilon_{\mathrm{s}}}{\bar{\varepsilon}}\right)^2\bar{c}\bar{\Phi}\geqslant 0$, where $\xi\equiv a/(3v\bar{\Phi})^{1/2}$ is the decay length in the absence of salt. Since $\frac{B}{\bar{\varepsilon}}\equiv\frac{Z^2e^2}{2a\bar{\varepsilon}kT}\frac{1}{1+\bar{\kappa}a}>>1$ (as checked using reasonable estimates of the different parameters), we may conclude: (i) high electrolyte concentration $\bar{c}$ favours phase separation of the polymer solution; (ii) multi-valent ions ($Z>1$) are much more effective in inducing phase separation (the lowering of solvent quality roughly decreases as Z^+ provided $B/\bar{\varepsilon}>>1$); (iii) salt-induced phase separation is easier for polymers less polar than the solvent. All these predictions are empirically well-known [30, 31].

"Solvation transitions"?

The likely occurrence of "solvation transitions", namely sudden variations of the solvation energy for certain critical parameters, is an attractive feature of the present model. The phenomenon shares strong similarities with the hydrodynamic instability in stratified fluid layers under a gravitational field. Convective instabilities arise when a denser fluid is placed on the top of a less dense fluid. Gravity tends to reverse the initial layered distribution, determining the onset of convective motions above a critical threshold related to the field strength and fluid–fluid interfacial tension [32].

In the case studied here (polymer chains less polar than solvent), a polymer-rich layer is spontaneously formed at the solute–solution interface at low surface charge density. In the case of PEG–water mixtures such a conjecture has been verified by surface pressure [33] and neutron reflection measurements [34] at the air–polymer solution interface, which clearly evidence interfacial polymer adsorption. Because of the lower solubility of the electrolytes in polymer-rich regions, ions are pushed far away from the uncharged (or slightly charged) surface (Eq. 37), as found by neutron data [34] and inferred from the salt effect on the surface pressure [35]. The effect accompanying salt depletion at the interface is the enhanced polymer adsorption on increasing the electrolyte concentration, a result theoretically predicted (Eq. 38) and experimentally found [33, 34, 35].

However, on increasing the solute charge density σ, the electrolytes are strongly attracted by the interface. The system becomes unstable: there is a huge electrolyte flux towards the interface accompanied by a backward flux of polymer towards the bulk because of partial incompatibility between ions and polymer. At high σ values the interfacial polymer concentration may become very small (Eq. 48) determining a consequent *increase* of the solution surface tension (the last two terms of Eq. 54). This is in sharp contrast to the low σ case where the surface tension *decreases* (the last two terms of Eq. 53). Indirect evidence of polymer (PEG) depletion near strongly charged interfaces has indeed been reported in the literature [36, 37, 38]. A cartoon of the above described scenario is given in Fig. 1 where we show both the ideal case (a) uniform polymer distribution, and the non-ideal case (b) coupled polymer–electrolyte distribution.

As shown in the theoretical section (see Eq. 49), the change between these opposite situations is not continuous but it may occur through a first-order phase transition. We do not expect, however, dramatic effects in the total solvation energy and related properties like solubility. In fact, the two energy minima, corresponding to a polymer-rich or an electrolyte-rich solute–solvent boundary layer, are qualitatively similar in energy. The polymer-rich boundary layer is stabilised by a smaller cavitation energy but it suffers from a more unfavourable electrostatic energy; on the contrary, the electrolyte-rich solvation layer is stabilised by a far greater electrostatic attraction but the cavitation energy is enhanced by a greater surface tension of the polymer solution. The balance between the compensating electrostatic and cavitation energies strongly reduces the possibility of observing discontinuities when plotting thermodynamic properties like, for instance, solubility data or solvation heats as a function of polymer concentration or solute charge density. Other phenomena, like chemical reactivity at solid–fluid interfaces or spectroscopic properties of interfacial molecules which probe local properties, should be more sensitive to the electrolyte/polymer concentration reversal on increasing the electrostatic potential.

A much simpler behaviour is predicted when the polymer is more polar than the solvent. In that case, even at low, or zero, solute surface charge density σ the first solvation layer contains more electrolyte than polymer. With rising σ there is a monotonous increase of electrolyte and a decrease of polymer concentration. The situation therefore resembles the stable configuration of a lighter fluid layer placed on the top of a heavier layer.

Failure of the classical partitioning of the solvation energy

The partitioning of the solvation energy into electrostatic and cavitation contributions is a fairly valid approximation in simple one-component solvents. Such an energy partition scheme is believed to be still valid in the case of complex fluid mixtures. We have proven, however, that this approximation might be totally incorrect in some cases. A careful analysis of the simple (but very approximate) equations here developed suggests that, even at small surface potentials, the electrostatic contribution to the total solvation energy decreases with the interfacial tension of the polymer solution (as described by the K_{eff}-dependent contribution in the first term of Eq. 53).

A more dramatic coupling is evident at high surface charge density. Here the indirect effect of the electrostatic potential counter-balances and may even reverse the polymer-induced lowering of the interfacial tension (see the fourth term in Eq. 54). On the contrary, the electrostatic contribution is strongly favoured by the potential-related increase of the polymer interfacial tension (the second term in Eq. 54).

Another consequence of the interplay between electrostatic solvation energy and cavitation (or solvophobic) forces in polymer + electrolyte solutions appears in the effect of salt concentration. At zero (or low) solute charge density σ, salt *decreases* the surface tension [34, 35], partially mitigating the well-known increase of the electrolyte solution surface tension with salt concentration in the absence of polymer [27, 28, 29] (water-soluble polymers are indeed known to protect proteins against salting-out properties of electrolytes [39, 40]). Because of the strong coupling between electrostatic and solvophobic forces the above effect is no longer true at high σ: the surface tension of polymer + electrolyte solution now *increases* with salt concentration (the last two terms of Eq. 54: $\frac{1}{kT}\gamma_S(\bar{\Phi}) \approx \frac{1}{kT}\gamma_S|_{\bar{\Phi}=0} + \frac{a^2\bar{\Phi}}{9\xi_{\mathrm{eff}}}\left(1 + 2\left(\frac{\xi_{\mathrm{eff}}}{\xi}\right)^2\right)$), the salt dependence being contained in the parameter ξ_{eff} defined by Eq. 53.

Concluding Remarks

In this work we have proposed a simple continuum approach to describe the solvation energy of large charged particles suspended in a semi-dilute polymer–electrolyte solution. At variance with earlier papers, we do not consider *any* direct interaction between solute surface and polymer. The calculated variations in the polymer profile (and in the related solvation energy) are the result of the mutual polymer–electrolyte partial exclusion. The ability of the model to qualitatively predict and explain several effects is self-evident. As it stands, however, the theory seems to be of little utility in quantitative predictions for real systems. Some approximations have been introduced just to obtain a physical insight into the phenomenon and could be removed at the expense of heavier mathematical complexity, while others deserve a more careful analysis. A crucial limit of our model is the solute geometry, that has been restricted to the case of an idealised flat infinite surface. While the adopted picture of semi-dilute polymer solutions forced us to consider large solutes, curvature effects could be introduced by exploiting the different scale lengths. On a large scale curvature effects can be considered through a systematic perturbation expansion in terms of the inverse curvature radius $1/R$ (present results are valid at $R \to \infty$). This job has indeed been performed for polymers near curved surfaces [41, 42] and can be easily extended to the polymer + electrolyte system here considered.

On an atomistic scale all surfaces are rough. The majority of recent solution theories have stressed the importance of a careful description of the solute–solvent interface in calculating the solvation energy [1, 2, 3]. While the electrostatic contribution described by the Poisson–Boltzmann equation (Eq. 25) could also be obtained in the case of an irregular surface, the coupled polymer distribution (Eq. 23) could not. However, polymer correlation length ξ_{eff} and surface roughness size D have in general different scales, for roughness of

the order of molecular diameters $\xi_{\text{eff}} > > D$. Therefore, near the solute surface the polymer concentration decays slowly, being nearly constant near the interface. Atomic-scale roughness can then be inserted into the model through an averaged boundary condition to the differential equation (Eq. 23). This procedure allows one to retain the simple analytical structure for the polymer distribution function far from the surface.

Much work is still needed to build-up a quantitative model of multi-component polymer solvents and more questions have been opened than solved by the author. It is our hope that useful hints could arise from this work.

Acknowledgements. This work has been partially supported by the Italian MIUR.

References

1. Cramer CJ, Truhlar DG (1996) In: Tapia O, Bertran J (eds) Solvent effect and chemical reactivity. Kluwer, Dordrecht
2. Tomasi J, Persico M (1994) Chem Rev 94:2027
3. Langlet J, Claverie P, Caillet J, Pullman A (1988) J Phys Chem 92:1617
4. Chitra R, Smith PE (2001) J Phys Chem B 105:11513
5. Chandra A (1998) Chem Phys 238:285
6. Acree WE, Tucker SA, Wilkins DC (1993) J Phys Chem 97:11199
7. Schatz TR, Kobetic R, Piotrowiak P (1997) J Photochem Photobiol 105:249
8. Huddleston JG, Willauer HD, Griffin ST, Rogers RD (1999) Ind Eng Chem Res 38:2523
9. Lentz BR, Lee JK (1999) Mol Membr Biol 16:279
10. Hui SW, Kuhl TL, Guo YQ, Israelachvili J (1999) Colloid Surf 14:213
11. Kleideiter G, Nordmeier E (1999) Polymer 40:4013
12. Kulkarni A, Zukoski C (2001) J Cryst Growth 232:156
13. Sear RP (1997) Phys Rev E 56:4463
14. Louis AA, Bolhuis PG, Meijer EJ, Hansen JP (2002) J Chem Phys 116:10547
15. de Gennes PG (1979) Scaling concepts in polymer physics. Cornell University Press, Ithaca
16. Tang H, Freed KF (1991) J Chem Phys 94:6307
17. Szleifer I, Widom B (1989) J Chem Phys 90:7524
18. Robinson RA, Stokes RH (1959) Electrolyte solutions. Butterworths, London
19. Zaslawsky BY, Miheeva LM, Rodnikova MN, Spivak GP, Harkin VS, Mahmudov AU (1985) J Chem Soc Faraday Trans I 85:2857
20. Vergara A, Paduano L, Sartorio R (2002) Macromolecules 35:1389
21. Smirnov VI (1975) Course de mathematiques superieures, vol IV. MIR, Moscow
22. Israelachvili JN (1990) Intermolecular and surface forces. Academic, London
23. Landau LD, Lifshitz EM (1980) Electrodynamics of continuum media. Pergamon, London
24. Davydov AS (1991) Solitons in molecular systems. Kluwer, Dordrecht
25. Abramowitz M, Stegun IA (1972) Handbook of mathematical functions. Dover, New York
26. Gradshteyn IS, Ryzhik IM (1980) Tables of integrals, series and products. Academic, London
27. Weissenborn PK, Pugh RJ (1996) J Colloid Interface Sci 184:550
28. Markin VS, Volkov AG (2002) J Phys Chem B 106:11810
29. Bostrom M, Williams DRM, Ninham BW (2001) Langmuir 17:4475
30. Boucher EA, Hines PM (1976) J Polym Sci 14:2241
31. Florin E, Kjellander R, Erikson K (1984) J Chem Soc Faraday Trans I 86:2889
32. Chandrasekhar S (1961) Theory of hydrodynamics stability. Pergamon, Oxford
33. Kuzmenka D, Granick S (1988) Macromolecules 21:779
34. Rennie AR, Crawford RJ, Lee EM, Thomas RK, Crowley TL, Roberts S, Qureshi MS, Richards RW (1989) Macromolecules 22:3466
35. Kuzmenka D, Granick S (1987) Polym Commun 29:64
36. Arnold K, Zschoering O, Barthel D, Herold W (1990) Biochim Biophys Acta 1022:303
37. Evans E (1989) Macromolecules 22:2277
38. Kuhl T, Guo YQ, Alderfer JA, Berman A, Leckband D, Israelachvili J, Hui SW (1996) Langmuir 12:3003
39. Curtis RA, Ulrich J, Montaser A, Prausnitz JM, Blanch HW (2002) Biotechnol Bioeng 79:367
40. Curtis RA, Steinbrecher C, Heinemann M, Blanch HW, Prausnitz JM (2002) Biophys Chem 98:249
41. de Gennes PG (1990) J Phys Chem 94:8407
42. Brooks JT, Marques CM, Cates ME (1991) J Phys (France) 1:673